Anomalous Packing in Thin Nanoparticle Supercrystals

D. Zanchet,[1,2] M. S. Moreno,[1] and D. Ugarte[1,*]

[1]*Laboratório Nacional de Luz Síncrotron (LNLS), C.P. 6192, 13083-970 Campinas-SP, Brazil*
[2]*Instituto de Física Gleb Wataghin, UNICAMP, C.P. 6165, 13081-970 Campinas-SP, Brazil*

(Received 28 January 1999)

We report a structural study of gold nanoparticle supercrystals formed by a few layers and of micrometer size, where the long-range order has been stimulated by a soft thermal annealing. We have clearly identified an expansion of the first layer lying on amorphous carbon substrate and an ordered second layer sitting on twofold saddle points. The third nanoparticle layer recovers the conventional close-packed stacking. This anomalous packing has been explained by means of a simple theoretical model based on dispersional forces. [S0031-9007(99)09432-6]

PACS numbers: 61.46.+w, 81.05.Ys

Nanosystems allow the generation of an extremely rich family of advanced materials of great technological significance. Among them, nanoparticles (NPs) are particularly interesting as they can be used as building blocks for novel functional materials. Mesoscopic systems, constituted by a regular assembly of clusters, are attractive because they would allow the control and exploitation of both individual and collective responses, although some complicated procedures may be required due to intrinsic difficulties of manipulating matter at nanometer scale.

Colloidal nanoparticles are very well suited for such application, since they can be easily synthesized with high yield and narrow size distributions [1–4], showing a tendency to form two-dimensional (2D) or three-dimensional (3D) crystals (NSCs). Many studies have already reported these remarkable properties for a wide range of materials, covering metals, oxides, semiconductors, etc. [5–14].

Although a great deal of scientific and technological work is at present being addressed to the generation of self-assembled NSCs, the experimental approach remains highly empirical. An interesting procedure relies on the use of external constraints such as the formation of Langmuir-Blodgett films [15,16]. A few studies have dealt with the basic interactions governing a self-assembly process, such as van der Waals particle interaction [17], polarizability of the solvent [18], thiol bundling [19], etc. In spite of these efforts, achieved crystal sizes are still in the sub- or micron range, frequently requiring transmission electron microscopes (TEM) or scanning probe microscopes to be studied. It is likely that technological applications will also require a controlled deposition of nanoparticle arrays formed by a few layers, where the substrate could play an essential role on the deposition, structure, and growth of NSCs [20].

In this Letter, we report structural studies of NSCs formed by an increasing number of NP layers (1–3). We have analyzed the case of dodecanethiol-passivated gold particles lying on amorphous carbon subjected to a soft thermal treatment. TEM images have revealed the formation of anomalous NP packing: expansion of the first layer and occupancy of saddle points by the second one; the third nanoparticle layer recovers the conventional close-packed (CP) stacking. The detection of these effects may have been hindered by the fact that previous studies dealt mainly with single-layer or thick ($\approx$5–10 layers) NSCs, where cubic CP structure (fcc) is usually favored [5]. We anticipate that these results will allow a more precise control of NP arrays for application on nanoelectronics.

Thiol-capped gold nanoparticles have been synthesized by the method proposed by Brust [21] with Au:S molar ratio of 4:1, yielding a mean particle diameter of 4.1 nm (FWHM $\approx$ 1.1 nm, determined by TEM [22]). Although the diameter distribution seemed to be quite narrow, spontaneous formation of ordered arrays was not observed when solution drops were deposited and dried at ambient conditions. In contrast, drying the colloid on a hot substrate (70–100 °C) has given rise to 2D and 3D ordered NP arrangements. We have limited the temperature to less than 100 °C, since above this value thiol molecules start to desorb from gold surfaces [23].

In order to enhance particle diffusion and organization, we have performed a further annealing process (12–24 h at 80 °C in toluene vapor). In this case, low magnification TEM inspection revealed that the NP arrangement had been substantially modified. The induced changes may be briefly described as an important reduction of the area covered by NP monolayers (2D), and the appearance of compact islands formed by the stacking of several layers. An example is presented in Fig. 1, where the progressive darkening from the border to the island center indicates an increasing thickness.

The outer and brighter island region (noted 1-L) displays the typical hexagonal CP array expected for a NP single layer, with an interparticle distance of $a_1 = (6.2 \pm 0.3)$ nm. This 1-L region is rather reduced ($\approx$10–20 nm), being formed by just 2–4 clearly visible individual NPs. Moving to the island center, it is possible to distinguish two different regular and well-defined contrast patterns. First, we can identify a hexagonal arrangement of white

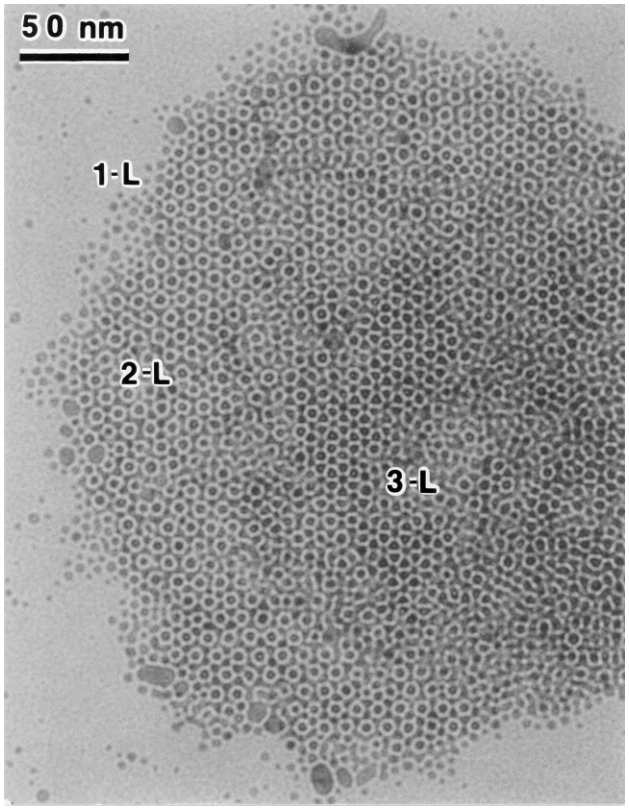

FIG. 1. TEM image of dodecanethiol-passivated gold nanoparticles on amorphous carbon film. Note the ordered arrangement and different regular contrast patterns that are easily discernible (1-, 2-, and 3-L regions).

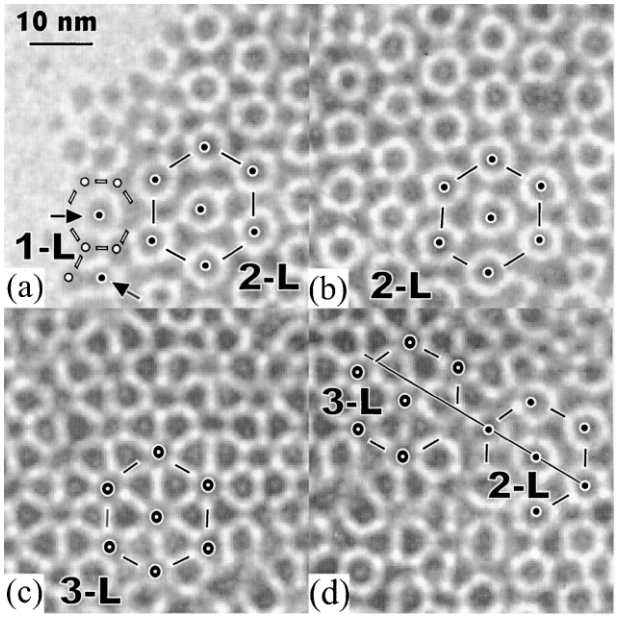

FIG. 2. Closer view of selected regions from Fig. 1: (a) NSC border showing the transition from the 1-L to 2-L regions; (b) 2-L zone; (c) central and thickest region (3-L); (d) transition between the 2-L and 3-L domains. Note that both hexagonal patterns in (d) have the same orientation and lattice parameter but are not aligned (a black line was drawn for comparison). See text for explanations.

rings (2-L zone) with a center-to-center distance $b_2 = (10.8 \pm 0.2)$ nm. Second, the island center displays another hexagonal pattern (3-L zone) composed of black dots surrounded by six dark triangles with an interdot distance (b_3) identical to the interring one (b_2).

Since three distinct ordered zones are observed going from the border to the island center, we infer that the image represents a NSC formed by a progressive superposition of 1, 2, and 3 layers. However, this assignment leads to a troublesome point: the usual CP NSCs (hexagonal or cubic) cannot account for the observed image contrast. In order to understand the NP packing generating the experimental image, we analyzed in detail both homogeneous and transition regions (Fig. 2).

The first and simplest feature, which we can derive from Fig. 2(a), is the existence of a 30° rotation between the hexagonal patterns of the 1-L and the larger hexagons of the 2-L region. Here, we indicate an extrapolation of the 2-L lattice (marked with arrows) into the 1-L region in order to emphasize the existence of a register between both motifs. As for the thicker regions, it is possible to observe that the 2-L and 3-L show hexagonal patterns of identical periodicity and orientation [Figs. 2(b) and 2(c)], but slightly shifted [$\Delta x \approx 3$ nm, Fig. 2(d)].

At this point, it is worth looking at the already reported NP ordered structures. Several groups have performed extensive studies of NSC [1,5–8,24,25] composed of thiol-capped noble metal particles. At present, it is well accepted that these NPs form hexagonal CP 2D layers, and the 3D NSCs display most frequently a fcc structure [Fig. 3(a)]. From these facts, it is inferred that NSCs can be approximately described in terms of hard spheres [24]. However, CP structures can explain neither the observed bright ring contrast [Fig. 2(b)] nor the measured rotation of hexagonal patterns from 1-L and 2-L regions [Fig. 2(a)]. It has also been reported that in a few cases, particles in a second stacked layer sit in twofold saddle points [marked *D* in Fig. 3(b)] instead of occupying the threefold hollow sites expected for CP structures [marked *B* or *C* in Fig. 3(a)]. However, for this case, no long-range order has yet been observed [25]. Indeed, a closer inspection of the 2-L region (Fig. 4) demonstrates unambiguously that the observed bright rings are generated by an ordered arrangement of NPs at twofold saddle points. The present experimental results indicate that the provided soft thermal treatment has allowed the formation of extended ordered 2-L regions, typically with several microns in size. Consequently, it follows that these saddle sites should be energetically favored in the studied system (two NP layers on *a-C*), in contrast to what is expected for hard spheres.

From a structural point of view, the suggested structure could be described as a $(\sqrt{3/2} \times \sqrt{3/2})R30°$ reconstruction, implying a second layer interparticle distance $a_2 = a_1 \cos 30°$ (= 5.4 nm). A structural model for the

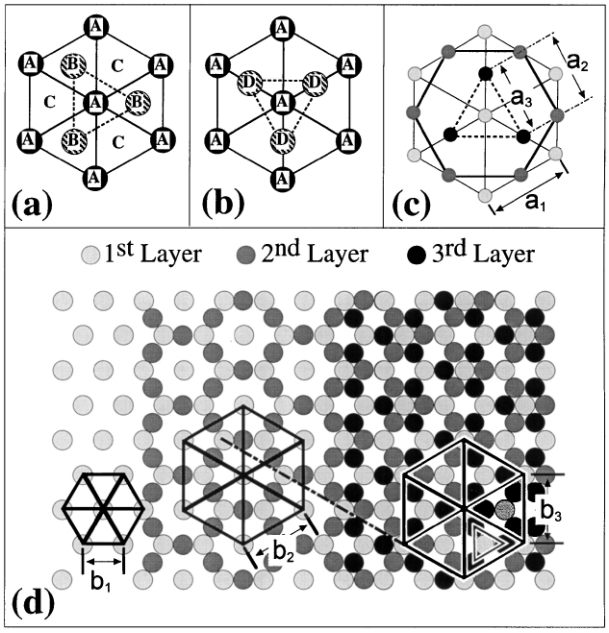

FIG. 3. Model structure for the 3-layer NSCs: (a) typical stacking sequence for CP structures; (b) alternative stacking sequence, where second layer particles occupy twofold saddle points (D); (c) 3-layer NSC stacking and corresponding interparticle distance for each layer; (d) bidimensional projection of the deduced thin crystal NP arrangement. In (d), the hexagonal patterns that can be directly associated to the experimental image are indicated by solid lines (lattice parameters b_1, b_2, and b_3). The dashed line has been drawn to indicate the shift between the two larger hexagons.

2-L region is presented in Fig. 3(d); for simplicity we have not included in this schema the NP sitting in an on-the-top position in the ring center. Although we do not dispose of experimental evidence to exclude these particles, intuitively, this position should be much less energetically favorable than the saddle or hollow sites.

Neglecting diffraction and focusing effects, the image contrast can be approximately associated to the projected potential of the sample, or even more easily to the thickness traversed by the electrons. The understanding of the 1-L contrast is straightforward with black dots representing the NP positions ($b_1 = a_1$). As for the two stacked layers in Fig. 3(d), the NP distribution leaves an uncovered substrate area with a ring shape, which has a periodicity ($b_2 = 2a_1 \cos 30°$; calculated value 10.7 nm) and a hexagonal arrangement in very good agreement with the experimental image. The proposed packing also reproduces the rotation of the hexagonal networks from 1-L and 2-L regions [Fig. 2(a)]. We remark that this rotation cannot be reproduced by an inversion of the first and second layers, resulting in an unambiguous determination of lattice parameters ($a_1 > a_2$) for the NP successive layers.

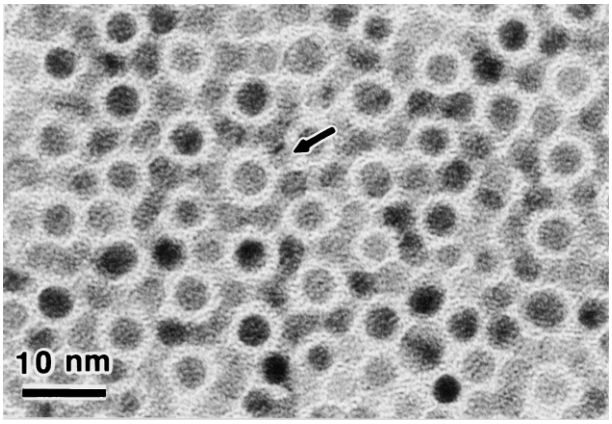

FIG. 4. Higher magnification TEM view of the NP positions in the 2-L region, where we can observe the occupancy of twofold saddle points (a clear example is marked with an arrow).

It must be emphasized that the model discussed above implies that the interparticle distances in the first and second layers are quite different ($a_2/a_1 = \cos 30°$). Recently, Korgel *et al.* [24] have proposed an effective hard sphere diameter (a_e) for thiol-capped metal particles as $a_e = d_m + t_{\text{th}}$ (d_m, metal core diameter; t_{th}, thiol thickness). The shorter interparticle distance, a_2, is in very good agreement with these results, since dodecanethiol contributes with an effective thickness of 1.5–1.8 nm. This enables us to adopt a_2 as the effective NP diameter, and, as a consequence, it reveals a lattice expansion of 15.5% of the NP layer in contact with the substrate.

The observation of an ordered NP array generated by the twofold saddle sites occupation raises a natural question about how this is related to the frequent observation of thicker NSCs displaying CP structure. It is very interesting to look at sites occupied by the third NP layer, which, however, requires a more detailed analysis. The contrast in the 3-L region displays two kinds of local 2D symmetries: threefold and sixfold that should be reproduced by the projected potential of the proposed model. Based on the fact that thicker NSCs should present a fcc structure, a reasonable estimate would be a third layer with a lattice parameter identical to the second one ($a_3 = a_2$) and CP stacking [Fig. 3(a)]. This simple approach produces a NP arrangement in very good accordance with the experiments. The final model is presented in Fig. 3(d), and the interparticle distances (a_1, a_2, and a_3) and the consecutive layer orientations are presented in Fig. 3(c). Although in this case it is certainly more difficult to make a straightforward association with the image contrast, the structural model does reproduce all the basic image characteristics: (a) local symmetries; (b) lattice parameters, $b_3 = b_2$; (c) hexagonal network orientation and shift ($\Delta x = a_1 \sin 30°$; calculated value 3.1 nm). In brief, despite the anomalous stacking of the second layer, the third one recovers the expected stacking. Extrapolating these results, we estimate the deposition of further NP layers will generate a fcc NSC of interparticle distance a_3 ($= a_2$) that we have already deduced as the effective hard sphere diameter.

The quantitative understanding of the energetics involved in the assembly and self-organization of

NSCs is still in its early stages [17,18], and a detailed analysis of the involved energetic factors would illuminate important issues for nanotechnology. Recently, Ohara *et al.* [17] have shown that size segregation (formation of opals) in dodecanethiol-stabilized gold nanocrystals is due to van der Waals interaction between particles described by the Hamaker potential [26]. Based on these results, we have used this potential (Hamaker constant of 1.95 eV [17]) to estimate the energy of saddle and hollow sites on a hexagonal CP NP layer using the simple configurations shown in Figs. 3(a) and 3(b). The particle size for steric repulsion was taken as the effective hard sphere size ($a_e = a_2$), and we included all intra- and interlayer interactions between particles. Calculations show that the occupation of hollow sites is favored by only $\approx$3 meV (0.1 kT) when compared with saddle sites. Considering the elementary approximations used, the results are very encouraging. It must be emphasized that the internal interaction between the second layer particles is the most relevant fact leading to a reduction of the system energy. In other terms, as the first layer is expanded (interparticle distance $> a_e$), the second layer can reduce the total energy by avoiding hollow sites that keep NPs farther apart than their effective diameter. Then, the twofold saddle point allows NPs to be closer and reduces the system energy; this fact has been verified by performing lattice dependent calculations.

We must point out that, in a strict sense, the NSCs studied in this work are quite different from previous ones, as we have subjected our NSCs to a thermal annealing. We may deduce that this treatment modifies in some way the NP-substrate interaction (e.g., NP mobility, adhesion, etc. [20]) giving the necessary conditions for the NP rearrangement and generating the unexpected long-range ordering of NPs in saddle sites.

In summary, we have been able to reveal and model the anomalous NP stacking during the first growth steps of NSCs on *a-C* substrates subjected to a soft thermal treatment. We have clearly identified two effects: (a) first layer expansion leading to a lattice parameter larger than effective NP hard sphere diameter; (b) second layer twofold saddle sites become energetically favored. We expect that these new results may be used to tune the NP array parameters by means of an appropriate modification of substrate properties.

We thank FAPESP (Contracts No. 96/12550-8, No. 97/4236-4, and No. 98/6667-5), CNPq, and LNLS for financial support. Electron microscopy studies were performed at CIME-EPFL, Lausanne, Switzerland (Philips EM-430T) and Centro de Microscopia Eletrônica-UFGRS, Porto Alegre, Brazil (JEM-2010 ARP).

*To whom correspondence should be addressed.
Electronic address: ugarte@lnls.br

[1] R. L. Whetten *et al.,* Adv. Mater. **8**, 428 (1996).
[2] M. M. Alvares *et al.,* Chem. Phys. Lett. **266**, 91 (1997).
[3] A. A. Guzelian *et al.,* J. Phys. Chem. **100**, 7212 (1996).
[4] C. B. Murray, D. J. Norris, and M. G. Bawendi, J. Am. Chem. Soc. **115**, 8706 (1993).
[5] Z. L. Wang, Adv. Mater. **10**, 13 (1998).
[6] S. A. Harfenist *et al.,* J. Phys. Chem. **100**, 13 904 (1996).
[7] S. A. Harfenist *et al.,* Adv. Mater. **9**, 817 (1997).
[8] Z. L. Wang *et al.,* Adv. Mater. **10**, 808 (1998).
[9] J. S. Yin and Z. L. Wang, Phys. Rev. Lett. **79**, 2570 (1997).
[10] L. Motte *et al.,* Adv. Mater. **8**, 1018 (1996).
[11] L. Motte *et al.,* J. Phys. Chem. B **101**, 138 (1997).
[12] J. R. Heath, Science **270**, 1315 (1995).
[13] C. B. Murray, C. R. Kagan, and M. G. Bawendi, Science **270**, 1335 (1995).
[14] C. J. Kiely *et al.,* Nature (London) **396**, 444 (1998).
[15] J. H. Fendler, Chem. Mater. **8**, 161 (1996).
[16] J. R. Heath *et al.,* J. Phys. Chem. B **101**, 189 (1997).
[17] P. C. Ohara *et al.,* Phys. Rev. Lett. **75**, 3466 (1995).
[18] B. A. Korgel and D. Fitzmaurice, Phys. Rev. Lett. **80**, 3531 (1998).
[19] Z. L. Wang *et al.,* J. Phys. Chem. B **102**, 3068 (1998).
[20] W. D. Luedtke and U. Landman, J. Phys. Chem. **100**, 13 323 (1996).
[21] M. Brust *et al.,* J. Chem. Soc. Chem. Commun. **1994**, 801 (1994).
[22] D. Zanchet *et al.* (to be published).
[23] E. Delamarche *et al.,* Langmuir **10**, 4103 (1994).
[24] B. A. Korgel *et al.,* J. Phys. Chem. B **102**, 8379 (1998).
[25] J. Fink *et al.,* Chem. Mater. **10**, 922 (1998).
[26] H. C. Hamaker, Physica (Utrecht) IV **10**, 1058 (1937).